Char-bed burning rates—experimental results

Craig A. Brown, Thomas M. Grace*, Steve J. Lien, and David T. Clay*

Char-bed burning geometry was simulated in a laboratory furnace. The results should prove to be useful in optimizing the distribution of air and liquor within the recovery furnace.

Combustion in the recovery boiler furnace can be separated into two main areas: in-flight and char-bed combustion. Liquor burning on the walls can also be significant, depending on the firing strategy. During in-flight burning, a portion of the liquor's heating value is released as drops of liquor fall toward the bed or are entrained in the gas stream. This energy release can consist of volatiles combustion and/or heterogeneous char combustion. The remaining portion of the liquor's heating value is released on or near the char bed. This, too, can consist of volatiles and/or char combustion.

All currently designed black-liquor recovery furnaces use some combination of in-flight and char-bed burning. Maximizing the bed burning rates is thought to be one way to increase the capacity of existing units. This is based on the premise that reducing in-flight combustion will reduce carryover and exit-gas temperatures, both of which contribute to pluggage. Recent trends in firing strategy, namely stationary firing and an increase in the air supply to the lower furnace, seem to be directed at increasing the portion of the burning that occurs on the char bed. Although these trends seem logical, a better fundamental understanding of char-bed combustion is necessary if we are to answer the basic question: "How much combustion can or should be supported on the bed?"

In particular, information is required on char-bed combustion rates in a realistic burning geometry. Previous work on the chemistry of char-bed reactions (*1*, *2*) suggested that char burning rates are limited by the mass transfer of O_2. The focus of this study was to measure char burning rates in a laboratory system under conditions that simulate those found in recovery furnaces. The results are expressed as experimentally determined mass-transfer coefficients.

Brown is a research engineer, Weyerhaeuser Paper Co., Tacoma, Wash. 98477. Grace is a consultant, T.M. Grace Co., Appleton, Wis., 54912-0833. Lien is a research engineer, Institute of Paper Science and Technology, Atlanta, Ga. 30318. Clay is a chemical recovery consultant, James River Corp., Neenah, Wis. 54957-0899.

*Formerly a professor at the Institute of Paper Chemistry.

Experimental approach

Char-bed furnace

The primary tool used in this work was the IPC char-bed-burning furnace, shown schematically in **Fig. 1**. The combustion process is contained in a metal retort surrounded by electrical heating panels. The panels are capable of maintaining temperatures in the retort between 750°C and 800°C. Inside the retort, a char-retaining insert confines the char to a 10-cm × 20-cm cross section. Preheated air and nitrogen mixtures introduced through a slot jet sweep across the char surface. The slot jet is 20 cm in length, the same as the bed width. The width of the adjustable slot jet was set at 7.6 mm for all tests reported here. Skirts on either side of the gas jet confine it to the bed width. The gas supply was preheated to temperatures between 240°C and 260°C.

As the bed burns away, contact between the gas jet and the char is maintained by continuously moving the char tray upward using a variable speed drive. Drive speed is adjusted based on observation of the bed surface as seen through the viewport. The char tray can travel up 51 cm. At the top of its travel, about 8 cm of char remains in the tray.

Surface and subsurface bed temperatures were measured by three thermocouples connected to the char tray. They were vertically spaced about 15.2 cm apart. As the tray was driven up, the individual thermocouples passed sequentially through the burning char surface. The thermocouple outputs were logged every 5 s.

The char-bed furnace is connected to the in-flight section of the IPC process flow reactor (*3*). This is an electrically heated tower furnace with a height of 4.3 m and an inside diameter of 10.5 cm. Black-liquor drops are injected at the top of the in-flight module. They fall to the char-bed furnace through an upflowing hot-air stream. By the time they reach the char bed, they are normally in a dried and partially devolatilized state.

Preformed char beds

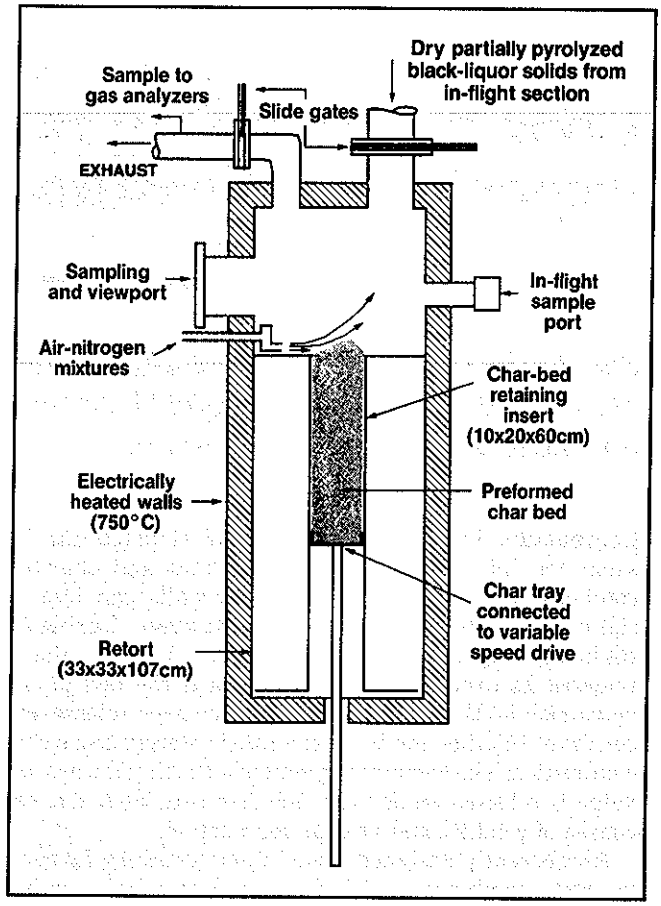
Bed burning was carried out in a batch mode. Char from the in-flight module was collected in the char-bed furnace under a nitrogen purge. It took about 30–40 min to fill the retaining insert with char. Since the furnace was

preheated to temperatures between 750°C and 800°C, the char continued to pyrolyze. When the char chamber was filled, the char feed was shut off and the char-bed furnace isolated from the in-flight module by means of a slide gate. Before starting an experimental burn, an additional 15 min was allotted to allow pyrolysis to be completed on the last char to arrive on the bed.

The burn was started by introducing a combination of air and nitrogen into the slot jet. Since all combustion gases exited through the furnace outlet pipe, it was possible to employ a simple material balance to determine burning rates. An extractive sampling system measured concentrations of CO, CO_2, O_2, and SO_2 in the outlet pipe. These values were logged every 20 s. The carbon consumption rate was calculated from CO and CO_2 concentrations and the outlet gas flow rate. The outlet gas flow rate was calculated from the measured inlet flow and a material balance on nitrogen. Fluxes were calculated based on the 10-cm × 20-cm bed cross section.

Every effort was made to produce a uniform and flat burning surface. In early tests, the tendency was to drive the char tray up too fast. This produced a very nonuniform burning surface. Rates measured during these tests were almost always significantly higher than later tests, when we had learned how to avoid overdriving the bed. The higher burning rates were attributed to the increased gas-char contact areas. Many of these earlier tests were dropped from the analysis because of the inability to quantify the contact area. Currently, videotape records are made of each test so that the constancy of the contact geometry can be verified.

1. Schematic of char-bed burning furnace



Char analysis

The chemical and physical characteristics of char beds formed by the previously described laboratory method were very reproducible for a given black liquor. The average chemical compositions and standard deviation values given in **Table I** are based on char samples taken prior to seven tests. The analyses are similar to those reported by Grace (*1*) for typical char from black-liquor pyrolysis. However, Table I shows that the losses for black-liquor solids and carbon are somewhat lower than those reported by Merriam (*4*) for recovery boiler char-bed samples. Analysis also showed that all organic carbon present in the laboratory char bed was fixed. This indicates that the char was completely pyrolyzed prior to burning.

Merriam's data showed a markedly greater char density than those found in our laboratory char beds, as much as one to two orders of magnitude difference. Direct measurement of our char density proved difficult. The values shown in Table I were calculated based on the integrated carbon release, initial carbon concentration, and char-retainer volume. This is representative of the overall bed density prior to the burn. Since we made no effort to mechanically densify the char, the density is similar to that of an agglomeration of swollen char particles.

This difference in densities is not surprising. In an actual char bed, the material just below the surface may be highly enriched in molten and/or solidified inorganic materials. By contrast, the laboratory char bed contains no molten inorganic material prior to burning. The density of the laboratory char bed does, however, increase steadily during the burn as smelt accumulates in the bed. Most of this increase is likely to be concentrated near the surface, since the subsurface temperatures were usually at or below the melting point of smelt.

The relative inability of smelt to flow down through the surface was supported by observation of the burning bed. For burns in air (highest burning temperatures), it appeared that the molten smelt was initially able to penetrate the surface. As the burn proceeded, penetration appeared to become more difficult. This effect was compounded by lower O_2 concentrations (lower bed temperatures). We also noted that once the burn was under way, gas velocities over the surface could be increased without entrainment of particles from the bed. However, even with the added density and improved adhesion provided by the molten inorganic material, maximum velocities were still limited by entrainment of char from the surface.

Test conditions

A list of the test conditions is given in **Table II.** All tests were conducted on char beds produced from a single source of black liquor. This liquor was selected because of its relatively low swelling characteristic, which provided somewhat denser beds and longer burn times.

I. Char composition summary

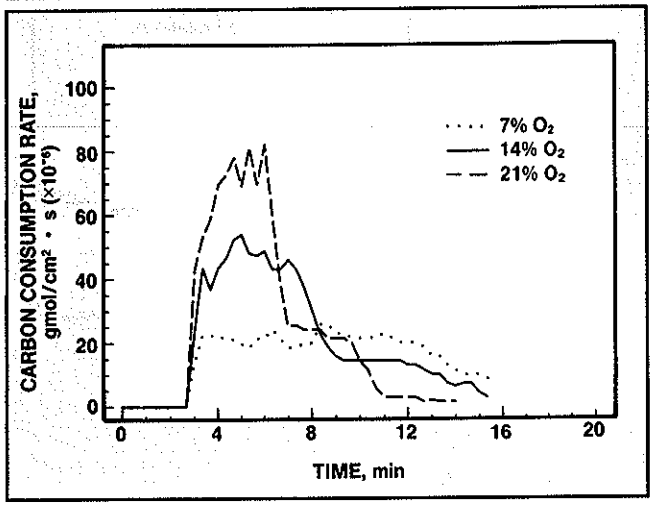
	Laboratory char beds (± std. dev.)	*Recovery boiler char beds*[a]
Elemental analysis, wt. %		
Sodium	29.2 ± 1.3	...
Carbon	24.9 ± 1.0	...
Hydrogen	0.57 ± 0.09	...
Oxygen	35.0 ± 0.4	...
Sulfur	4.2 ± 0.4	...
Losses summary,[b] %		
Solids	34.3 ± 3.1	45–55
Carbon	53.3 ± 2.2	75–85
Hydrogen	87.9 ± 1.7	...
Oxygen	36.4 ± 3.3	...
Sulfur	44.4 ± 5.4	...
Calculated values		
Reduction, %	52.6 ± 6.0	...
Bulk density, g/L	14.2 ± 2.3	300–1300
Higher heating value, kJ/kg	5260 ± 220	...

[a]From Merriam *et al.* (4). Losses calculated assuming typical liquor composition. [b]Calculated assuming no sodium loss.

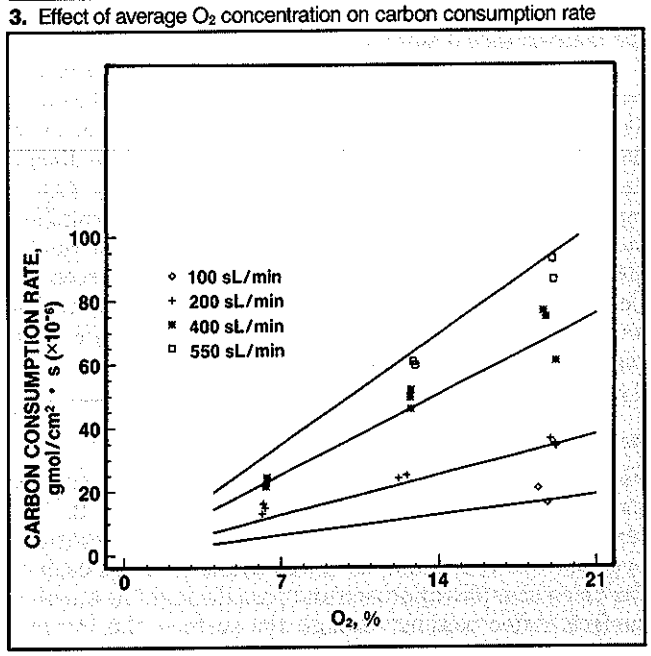
II. Test conditions

Inlet O_2, %	*Inlet gas flow, std. L/min*	*Number of tests*
7	200	3
7	400	2
14	200	2
14	400	3
14	550	2
21	100	2
21	200	3
21	400	3
21	550	2

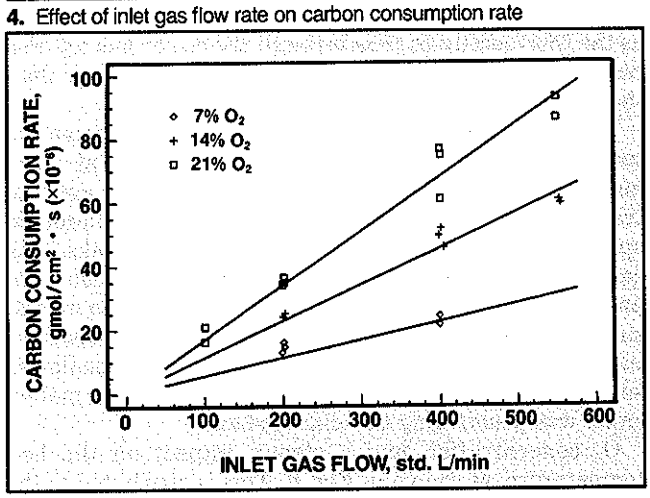
2. Carbon burn-up rate as a function of time. Gas flow rate = 400 std. L/min.



3. Effect of average O_2 concentration on carbon consumption rate



4. Effect of inlet gas flow rate on carbon consumption rate



Results

Burning rates

Figure 2 shows burning rate data from three typical tests. The most useful information is obtained from the relatively constant burning rate period at the start of each test. During this period, the bed is being driven up to maintain a constant gas-char contact area. Since the volume of char is fixed, the length of this period depends on the test conditions. For high O_2 concentrations and high gas flow rates, it was as short as 2 min. For low O_2 concentrations and low gas flow rates, some tests lasted longer than 15 min. Average burning rates from this constant-rate period are the primary output for each test.

Once the limit of bed travel has been reached, the rate begins to fall off. About 8 cm of char remains in the tray at this point. Once the surface has burned away from the gas jet, the rate levels off again, presumably controlled by the diffusion of O_2 to the receding char surface. The

rate falls off again when the char is almost consumed and the temperature drops.

The strong dependence of burning rate on O_2 concentration and gas flow rate are apparent in **Figs. 3 and 4**. The burning rates appear to be linearly dependent upon both O_2 concentration and gas flow rate. The linear dependence upon O_2 concentration is consistent with a mass-transfer-controlled process. As will be explained later, the apparent linear dependence on gas flow rate is also consistent with a mass-transfer-controlled process. A linear regression using the product of the O_2 concentration and the gas flow rate produced an r^2 value of 97%. This regression equation is depicted by the solid lines in Figs. 3 and 4.

Bed temperatures

Figure 5 shows bed temperature data obtained during the same three tests that were shown in Fig. 2. The temperatures start out at the furnace temperature, between 750°C and 800°C. Three peaks occur as each of the thermocouples approach and pass through the burning surface. After passing through the surface, the thermocouples are rapidly cooled by radiation to the furnace walls and by convection to the gas stream flowing over the bed. In the case of the low-O_2 burns (7% inlet O_2), the temperatures initially dip below the furnace temperatures as the thermocouples pass through the cooler gas jet. For burns in air, temperatures above the bed are higher than the furnace wall temperatures.

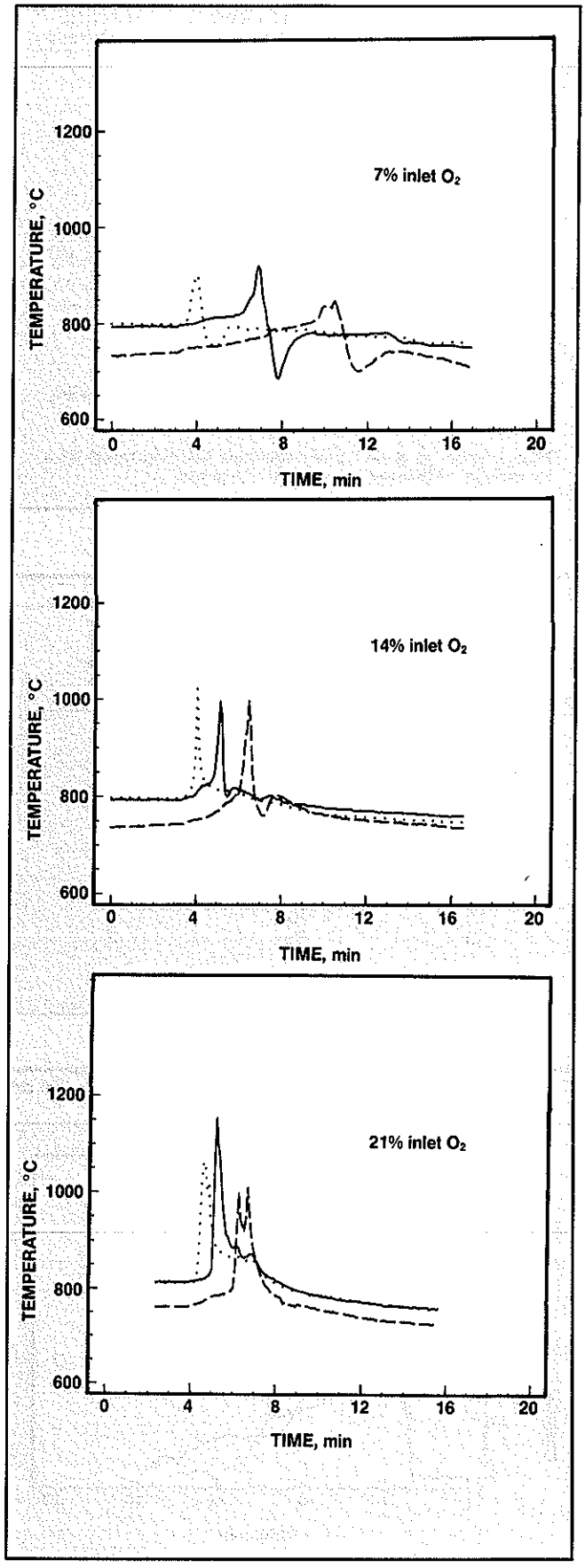
The depth of the active layer can be estimated from the temperature data in Fig. 5 by using the average tray speed and the rise time for the temperature peaks. The average tray speed is calculated using the known thermocouple spacing and the time between the temperature peaks. This calculation suggests that the active layer is between 3 cm and 7 cm deep. Part of the heating may be due to molten smelt flowing into the bed from the surface. However, particularly at the low and middle O_2 concentration (lower surface temperatures), it did not appear that the molten smelt was penetrating the char surface.

O_2 concentration had a strong impact on the bed temperature, as shown in **Fig. 6**. This is attributed to the increased heat-release rates at higher burning rates. The effect of gas flow rate was less pronounced. Although higher velocities increased burning rates through enhanced mass transfer, the effect on bed temperature was offset by increased convective cooling of the bed.

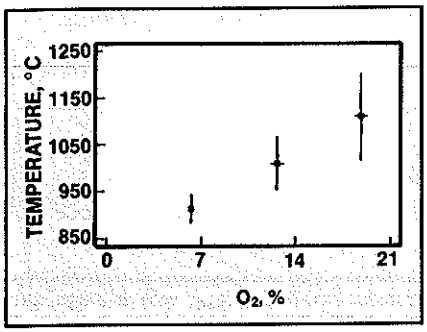
$CO/(CO_2 + CO)$ vs. O_2

For inlet O_2 concentrations below 14%, the fraction of CO [$CO/(CO + CO_2)$] in the off gases averaged about 50%, as seen in **Fig. 7**. For burns in air, the CO fraction dropped down to between 10% and 20%. A likely explanation for these phenomena is the temperature dependence of the rate of conversion of CO to CO_2 in the gas phase. For burns in air, the combustion heat release was sufficient to elevate the gas temperatures above the ambient furnace temperature, as seen in Fig. 5. Once the gas temperature is sufficient to promote conversion of CO to CO_2, the gas temperature is further elevated by the heat release from this reaction. Unlike burns at lower O_2 concentration, burns in air produced visible yellow-orange flames over the char surface. Aiken (*5*) observed a similar

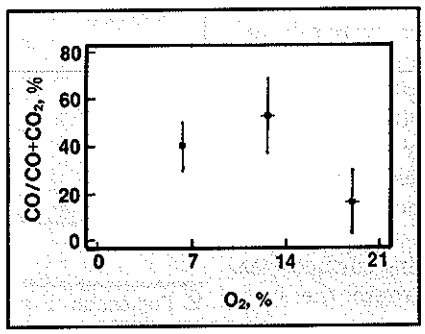
5. Thermocouple readings as a function of time. Peaks occur for top, middle, and bottom thermocouples (from left to right). Gas flow rate = 400 std. L/min.



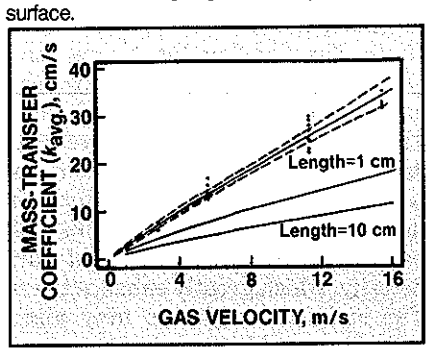
6. Effect of O_2 concentration on maximum bed temperatures (95% confidence intervals)



7. Effect of O_2 concentration on CO fraction in off gases (95% confidence intervals)



8. Average mass-transfer coefficient as a function of average gas velocity over char surface.



III. Parameters* for average mass-transfer-coefficient correlations with form $Nu_m = A + B(Re)^n Sc^{0.33}$

Configuration	Dimension for Reynolds number	A	B	n
Flat plate (laminar)	Plate length	0	0.664	0.5
Flat Plate (turbulent)	Plate length	0	0.036	0.8
Sphere	Diameter	2.0	0.60	0.5

*From Bird *et al.* (6).

temperature-dependent breakpoint for the gas-phase conversion of CO in his work.

Mass-transfer coefficient

Convective mass transfer is generally handled by analogy with heat transfer. Mass-transfer correlations generally take the form:

$$Nu_m = A + [B(Re)^n (Sc)^{0.33}] \quad (1)$$

where

Nu_m = kL/D, Nusselt number for mass transfer

Re = UL/ν, Reynolds number

Sc = ν/D, Schmidt number

k = mass-transfer coefficient

L = characteristic dimension

D = molecular diffusivity

U = free stream velocity

ν = kinematic viscosity

A, B, and n are experimental constants. The value of n is generally less than 1.0 and typically increases with increasing Reynolds number. Constants for correlations that might be applied to char-bed burning are given in **Table III.**

Based on Eq. 1 and Table III, we should expect the mass-transfer coefficients calculated for the laboratory burns to be dependent upon gas velocity raised to some power between 0.5 and 1.0. Changes in the gas film temperature will affect the diffusivity and viscosity. For the range of temperatures seen in the laboratory burns, these changes tend to offset each other.

Average mass-transfer coefficients, $k_{avg.}$, were calculated from the experimental burning rates as follows:

$$k_{avg.} = NO_2/\Delta c \quad (2)$$

Here NO_2 is the O_2 flux to the surface (gmol/cm^2·s) and Δc is the O_2 concentration gradient (gmol/cm^3). The O_2 concentration gradient was taken as a linear average of the inlet and outlet O_2 concentrations. This assumes the O_2 concentration at the char surface to be zero. The O_2 flux could have been calculated directly from the CO and CO_2 or O_2 measurements. However, this would include O_2 consumed in the gas-phase conversion of CO to CO_2 above the bed. Instead, we calculated the O_2 flux from the carbon flux and an assumed value for the fraction of carbon oxidized to CO [CO/(CO + CO_2)] during char burning. Based on the results presented earlier, this fraction was taken to be 0.5.

Gas velocities in the char-burning furnace were not measured directly. Instead, average gas velocities over the char surface were predicted from published correlations for the expansion of turbulent jets. The velocity over the char surface was taken as the centerline velocity of a slot jet with a nozzle width equal to twice the actual setting of 7.6 mm. In effect, this is equivalent to placing a plate along the center streamline of the jet and neglecting the viscous effects along the plate. Velocities calculated in this way are listed for the test conditions in **Table IV.**

The regression results in **Table V** indicate that the experimental data agree very well with the form of the theoretical mass-transfer expression given in Eq. 1. The r^2 values indicate that better than 94% of the variation in the data can be explained by a linear regression model. Fitting the data with a power model improved the correlation coefficient only slightly over that of the linear model. This is not surprising considering the relatively narrow range of velocities tested. Variations in velocity over at least one order of magnitude would be necessary to determine the exact power dependence. However, the "best fit" value of 0.91 does suggest that a square-root dependence is unlikely.

The experimental power-model correlation is plotted along with the theoretical correlation for a turbulent boundary layer over a smooth flat plate in **Fig. 8.** (Dashed

lines represent 95% confidence limits for the mean response.) Also depicted are the theoretical predictions for turbulent flow over flat plates with lengths of 1 cm and 10 cm. The plate lengths of 1 cm and 10 cm were selected to correspond roughly to the swollen diameter of a char particle and the laboratory char-bed length, respectively. The magnitudes of the theoretical coefficients are in reasonable agreement with the measured coefficients. It is not surprising that the measured coefficients are higher by a factor of 2 or 3. Much of this difference can probably be attributed to the effects of surface roughness and porosity, which greatly enhance the reacting surface area. The surface roughness may also increase the local turbulence and hence mass transfer.

Discussion

The trend toward firing strategies that increase burning intensity in the lower furnace provides a focus for two questions:

1. Are there limits to the amount of burning that can occur on a char pile?
2. How can bed burning rates be increased?

The data obtained in this study provide an opportunity to begin answering these questions.

Char burning in the laboratory furnace differs in some significant ways from bed burning in recovery furnaces. First, the surface of a real char bed may consist of partially devolatilized char and partially dried black liquor. Thus drying and pyrolysis may occur in parallel with char combustion on a real char bed. Secondly, in a recovery furnace, the bed surface is continuously replenished with fresh fuel from above. In our laboratory furnace, prepyrolyzed char of continuously increasing inorganic content refreshes the surface from below. Despite these complications, the basic O_2 mass-transfer-controlled char-burning process should be quite similar. It is useful to compare our experimentally measured burning rates with parameters for a recovery furnace.

The maximum experimentally measured burning rates occurred at the highest O_2 concentrations (21%) and the highest velocities. The experimental burning rates can be expressed as either a net flux of carbon gases away from the bed surface or as an O_2 flux to the bed. The maximum measured carbon consumption rate in the laboratory system was about 100×10^{-6} gmol/cm^2·s. The maximum O_2 flux to the bed can be calculated from the maximum carbon consumption rate using an assumed value of 0.5 (based on results presented earlier) for the fraction of carbon released as CO. This gives a value for the maximum measured O_2 flux of 75×10^{-6} gmol/cm^2·s.

A typical design rate for firing black-liquor solids in a recovery furnace, based on hearth area, is about 730 kg/h·m^2 (150 lb/h·ft^2). The amount of char carbon per unit hearth area can be calculated from this design value by assuming that the black-liquor solids are 35% carbon, by weight, and that 40% of this total carbon ends up as fixed carbon in the char. This gives a flux of 230×10^{-6} gmol/cm^2·s of char carbon based on hearth area. Thus, the maximum experimentally measured carbon consumption rate (100×10^{-6} gmol/cm^2·s) corresponds to about 45% of the char-carbon flux at recovery furnace design loadings.

IV. Calculated gas velocities in laboratory char-bed furnace

Inlet gas flow, std. L/min	Nozzle exit, Reynolds number	Gas velocities, m/s: Nozzle exit	Gas velocities, m/s: Average over bed
100	333	3.0	2.8
200	666	6.1	5.6
400	1331	12.2	11.3
550	1831	16.8	15.5

V. Regression of mass-transfer coefficient, $k_{avg.}$, with average gas velocity, U

Form	A	B	r^2	Std. error of estimate
$k_{avg.} = A + BU$	2.35	2.02	94.5	2.11
$k_{avg.} = AU^B$	2.78	0.91	96.1	0.10

This simple comparison suggests that about 45% of the char-carbon flux in a recovery furnace could be burned on the char bed.

The stoichiometric oxygen demand for black-liquor solids is typically about 0.9 kg O_2/kg black-liquor solids. At a design hearth loading of 730 kg/h·m^2 of black-liquor solids, the stoichiometric oxygen demand per unit hearth area is about 570×10^{-6} gmol/cm^2·s. This would be the O_2 flux to the bed if all of the burning took place directly on the bed. Thus, the maximum experimentally measured oxygen consumption rate of 75×10^{-6} gmol/cm^2·s corresponds to about 15% of the recovery furnace stoichiometric oxygen demand. This simple comparison suggests that about 15% of the recovery furnace burning load could be handled by combustion of char carbon on the bed itself. Note that the maximum O_2 rate calculated for the laboratory system does not include O_2 consumed in gas-phase reactions with CO and volatile combustibles immediately above the bed. These gas-phase reactions could represent a significant additional contribution to the burning load in the region of the bed.

The comparisons between the laboratory system and the recovery furnace implicitly assume that fuel and oxygen are uniformly distributed over the recovery furnace hearth. In practice, the O_2 concentrations over the char bed will vary from 21% close to the primary air ports to much lower values in the center. On the other hand, velocities near the primary air ports are expected to be 1.5 to 3 times higher than the maximum used in the laboratory system. Since the char burning rates increase with velocity in a nearly linear fashion, the higher velocities will somewhat compensate for the lower O_2 concentrations over the center of the bed.

The mass-transfer coefficients produced by this work should be useful in estimating the char-bed burning capacity. Estimates of the O_2 concentrations and gas velocities over the char bed could be used to calculate the char burning capacity in different regions of the char bed. More detailed models could predict O_2 concentrations, gas velocities, temperatures, and reduction efficiency over the

char-bed surface. Such an effort is currently underway at the Institute of Paper Science and Technology.

Conclusions

Reliable measurements of char-bed burning rates have been carried out in a laboratory environment. Burning rates were obtained under conditions that simulate char-bed burning in recovery boiler furnaces.

The burning-rate data are completely consistent with a burning process that is limited by mass transfer of O_2. The burning rate is directly proportional to O_2 concentration and dependent on velocity to a power between 0.8 and 1.0. Measured burning rates are of the approximate magnitude predicted by mass-transfer-coefficient correlations.

The data provide a quantitative estimate of the amount of burning that could take place on the char bed of a recovery furnace. It is not unreasonable to expect that about 45% of the char carbon could be burned on the char bed. This represents about 15% of the total burning load. These estimates may be further refined by use of the experimentally determined mass-transfer coefficients in models of the char bed.

Sharp thermal gradients exist between the reacting char surface and char only a few centimeters beneath the surface. The active burning layer is probably no more than 10 cm in thickness.□

Literature cited

1. Grace, T. M., Cameron, J. N., and Clay, D. T., Char Burning, summary technical report to the American Paper Institute, Project 3473-6, The Institute of Paper Chemistry, Appleton, Wis., 1985.
2. Thorman, R. P. and Macur, T. S., 1985 International Chemical Recovery Conference Proceedings, TAPPI PRESS, Atlanta, p. 451.
3. Clay, D. T. *et al.*, Fundamental Studies of Black Liquor Combustion, Report No. 2, Phase I (Oct. 1984–Dec. 1986), U.S. Dept. of Energy Report No. DOE/CE/40637-T2 (1987).
4. Merriam, R. L. and Richardson, D. L., Study of Cooling and Smelt Solidification in Black Liquor Recovery Boilers, Phase I report prepared for the American Paper Institute, New York, 1977.
5. Aiken, G. W., The use of a char pile reactor to study char bed processes, Ph.D. thesis, The Institute of Paper Chemistry, Appleton, Wis., 1988.
6. Bird, R. B., Stewart, W. E., and Lightfoot, E. N., Transport Phenomena, Wiley, New York, 1960.

This work was partially supported by funds from the Department of Energy under contract AC02-83CE40637 administered by Stanley F. Sobczynski. Additional support came from the Institute of Paper Science and Technology and its member companies. The support from these organizations is gratefully acknowledged. The support of the Weyerhaeuser Company by providing Craig Brown as an Industrial Research Fellow to IPSAT is also gratefully acknowledged. A special thanks is extended to Orlin Kuehl for his efforts in developing and operating the test equipment.

Received for review May 5, 1989.

Accepted June 21, 1989.

Presented at the 1989 International Chemical Recovery Conference.

INCREASE YOUR VISIBILITY!

Write A Paper For *Tappi Journal*

Your opportunities to get ahead in the pulp and paper industry depend on a number of factors — your education, your expertise, your ability to get along with people, your understanding of your markets and how your company fits into them. But the key to your advancement is your company's and colleagues' recognition of your knowledge and understanding.

That's why writing a paper for publication in *Tappi Journal* is important. The journal is considered the most authoritative publication serving the paper industry. When your paper is accepted for publication, you and your expertise become known to a large number of readers throughout the industry. Because they know that each paper the journal publishes is reviewed by working mill professionals recognized for expertise in their areas, readers know it's the best information available.

Increase your visibility. Advance your career. We'll make it easier with our free booklet, "Author Guidelines for Submitting an Article to *Tappi Journal*."



Tappi Journal • Technology Park/Atlanta
P.O. Box 105113 • Atlanta, GA 30348-5113
1-800-332-8686 U.S.A.
1-800-446-9431 Canada